Measurement of f_s/f_u Variation with Proton-Proton Collision Energy and B-Meson Kinematics

R. Aaij *et al.*[*]
(LHCb Collaboration)

(Received 22 October 2019; revised manuscript received 13 December 2019; accepted 2 March 2020; published 26 March 2020)

The ratio of the B_s^0 and B^+ fragmentation fractions f_s and f_u is studied with $B_s^0 \to J/\psi\phi$ and $B^+ \to J/\psi K^+$ decays using data collected by the LHCb experiment in proton-proton collisions at 7, 8, and 13 TeV center-of-mass energies. The analysis is performed in bins of B-meson momentum, longitudinal momentum, transverse momentum, pseudorapidity, and rapidity. The fragmentation-fraction ratio f_s/f_u is observed to depend on the B-meson transverse momentum with a significance of 6.0σ. This dependency is driven by the 13 TeV sample (8.7σ), while the results for the other collision energies are not significant when considered separately. Furthermore, the results show a 4.8σ evidence for an increase of f_s/f_u as a function of collision energy.

DOI: 10.1103/PhysRevLett.124.122002

The proton-proton (pp) collisions at the LHC produce copious pairs of b and $\bar{b}$ quarks, which immediately hadronize into the full spectrum of b hadrons. The knowledge of b-hadron production rates is crucial in order to measure their branching fractions.

The fragmentation fractions f_u, f_d, f_s, and f_{baryon} are defined as probabilities for a b quark to hadronize into a B^+, B^0, B_s^0 meson or a b baryon, respectively. (The inclusion of the charge-conjugate modes is implied throughout this Letter.) These include all possible contributions from intermediate states decaying to the mentioned hadrons via strong or electromagnetic interaction. The b-hadron fragmentation fractions were first measured in e^+e^- collisions at the Z resonance by LEP experiments [1–4] and in $p\bar{p}$ collisions at $\sqrt{s} = 1.8$ TeV center-of-mass energy by the CDF experiment [5]. In the absence of contradicting evidence, the fragmentation fractions determined in different collision environments were considered universal and averaged [6].

More recent measurements have shown that the hadronization fraction ratio $f_{\Lambda_b^0}/f_d$ depends strongly on the p_T and pseudorapidity of the produced b hadron [7–9]. Evidence has also been seen for a dependence on p_T^B of the relative B_s^0- and B^0-meson production f_s/f_d [10]. In combination with changes in the produced b-quark spectra, it could lead to modified fragmentation-fraction ratios at higher pp collision energies and therefore affect the branching fraction measurements which rely on normalization.

This analysis studies the relative B_s^0- and B^+-meson production f_s/f_u dependence on pp collision energy and on the kinematics of the produced b hadron. Measuring the relative production is not only important for the studies of underlying QCD, f_s/f_u represents also an essential input and a dominant source of systematic uncertainty in B branching-fraction measurements performed in hadron colliders, e.g., $B_s^0 \to \mu^+\mu^-$ [11,12].

The analysis is performed on four independent data samples collected with the LHCb detector at three pp collision energies: at $\sqrt{s} = 7$ TeV in the year 2011 (corresponding to 1 fb^{-1}), 8 TeV in 2012 (2 fb^{-1}), and at 13 TeV in the years 2015 (0.3 fb^{-1}) and 2016 (1.1 fb^{-1}). The relative production of B_s^0 mesons to B^+ mesons in the detector acceptance is measured in each sample with the ratio of efficiency-corrected yields of $B^+ \to J/\psi K^+$ and $B_s^0 \to J/\psi\phi$ decays

$$\mathcal{R} \equiv \frac{N(B_s^0 \to J/\psi\phi)}{N(B^+ \to J/\psi K^+)} \frac{\epsilon(B^+ \to J/\psi K^+)}{\epsilon(B_s^0 \to J/\psi\phi)} \propto \frac{f_s}{f_u}, \quad (1)$$

where $J/\psi \to \mu^+\mu^-$ and $\phi \to K^+K^-$. Here N denotes the selected and reconstructed candidate yield and ϵ is the related efficiency.

The study is further extended to the relative productions as a function of B-meson kinematic variables: momentum (p^B), transverse momentum (p_T^B), longitudinal momentum (p_L^B), pseudorapidity (η^B), and rapidity (y^B). (The longitudinal momentum component is the momentum component along the beam direction.) Because of the large uncertainty on the $B_s^0 \to J/\psi\phi$ branching fraction, no attempt is made to measure the absolute f_s/f_u value.

[*]Full author list given at the end of the article.

(In Ref. [13], the ratio $\mathcal{R}$ was converted to an absolute f_s/f_d value using a theoretical prediction for the ratio of the $B_s^0 \to J/\psi\phi$ and $B^0 \to J/\psi K^{*0}$ branching fractions [14]. In this Letter, Ref. [14] is not used due to disputed theoretical uncertainties arising from factorization assumption.) In the different context of light and strange hadrons, the ALICE experiment has observed a dependence of their production ratios on the multiplicity of the event [15–17]. In this analysis, this dependence is not studied, owing to technical reasons; however, such behavior will be the subject of future studies.

The LHCb detector [18,19] is a single-arm forward spectrometer covering the (final-state track) pseudorapidity range $2 < \eta < 5$, largely complementary to the other LHC experiments. The detector includes a high-precision tracking system consisting of a silicon-strip vertex detector surrounding the pp interaction region, a large-area silicon-strip detector located upstream of a dipole magnet, three stations of silicon-strip detectors, and straw drift tubes located downstream of the magnet. Particle identification is provided by two ring-imaging Cherenkov detectors, an electromagnetic and a hadronic calorimeter, and a muon system composed of alternating layers of iron and multiwire proportional chambers.

The online event selection is performed by a two-stage trigger and relies on muon candidate tracks. The first level (hardware) trigger decision is based on information from the muon systems and selects events containing at least one muon with a large p_T or a pair of muons with a large product of their transverse momenta ($\sqrt{p_T p_T'}$). The trigger thresholds vary between 1 and 2 GeV/c, depending on the data-taking conditions.

The second level (software) trigger reconstructs the full event, looks for dimuon vertices and requires them to be significantly displaced from any primary vertex (PV). At least one of the tracks must have $p_T > 1$ GeV/c and be inconsistent with originating from any PV. Only events in which the trigger decision was based on the muon tracks from the signal candidates are kept. The muon candidates are required to pass the muon identification criteria [20]. No additional particle identification is required on the kaon candidates.

Off-line, the J/ψ candidates are reconstructed by combining two oppositely charged muon tracks originating from the same vertex. The $\phi(1020)$ candidates are reconstructed from the decays to the K^+K^- final state. The $B^+ \to J/\psi K^+$ ($B_s^0 \to J/\psi\phi$) candidates are built by combining the J/ψ candidates with a K^+ (ϕ) candidate. Prompt combinatorial background is suppressed by removing the events in which the J/ψ vertex fit χ^2, B vertex impact parameter, or J/ψ vertex distance indicate that the decay vertex is either poorly reconstructed or close to the PV. No further selection is applied on the reconstructed ϕ vertex in order to minimize the differences between the two signal-channel selections. Only J/ψ (ϕ) candidates with mass within ± 60 MeV/c^2 (± 10 MeV/c^2) of the known J/ψ (ϕ) masses [6] are kept; these ranges are several times the mass resolutions of about 16 MeV/c^2(3.5 MeV/c^2).

Signal track candidates with momenta $p > 500$ GeV/c, transverse momenta $p_T > 40$ GeV/c, or pseudorapidity outside of the range $2 < \eta < 4.5$ are removed. In addition, muon and B transverse momenta are asked to pass $p_T > 250$ MeV/c and $p_T^B > 500$ MeV/c requirements, respectively. The selected sample covers the following B-meson kinematic range: $20 < p^B < 700$ GeV/c, $20 < p_L^B < 700$ GeV/c, $0.5 < p_T^B < 40$ GeV/c, $2.0 < \eta^B < 6.5$, and $2.0 < y^B < 4.5$. The η^B region between 2.0 and 2.5 is also accessible to the ATLAS and CMS experiments and thus important for comparison and combination of the results.

Simulated signal events are used to determine the detection efficiencies, estimate the background contamination, and model the mass distributions of the selected candidates. The simulated pp collisions are generated using PYTHIA [21] with a specific LHCb configuration [22]. Hadron decays are described by EvtGen [23] with final-state radiation generated using PHOTOS [24]. The particle interactions with the detector material and the detector response are implemented using the GEANT4 toolkit [25,26]. The samples of simulated signal events are corrected for known differences between data and simulation [27] in bins of detector occupancy and kinematic variables. When considering the B_s^0 over B^+ distribution ratio, the consistency between data and simulation before correction corresponded to a p value of at least 14% in the kinematic variables and exceeded 90% in the detector occupancy.

The signal yields are obtained by fitting the B^+- and B_s^0-candidate mass distributions, $m(J/\psi K^+)$ and $m(J/\psi K^+K^-)$, in the ± 100 MeV/c^2 range around the known mass values using independent extended unbinned maximum-likelihood fits. To improve the mass resolution, the B-candidate masses are computed with the J/ψ mass constrained to its known value [6].

The mass distributions are described with probability density functions (PDFs) consisting of signal, combinatorial background, and background due to pions or protons that are wrongly identified as kaons. The signal components are parametrized by Hypatia functions [28], which consist of hyperbolic cores and power-law tails on both sides. The values of the parameters that define the tails are determined from simulation. The combinatorial backgrounds in both models are described by exponential PDFs. The means and widths of the signal components and the slopes of the exponentials are unconstrained. The values obtained in the data are larger by 10% or less for the widths and are consistent for the means and the other shape parameters. The fits repeated with fixed tails in the signal shape give consistent yield results to the constrained fits used by default. The contribution due to misidentified $B^+ \to J/\psi\pi^+$ decays in the $m(J/\psi K^+)$ distribution is described using a kernel density estimator technique [29]

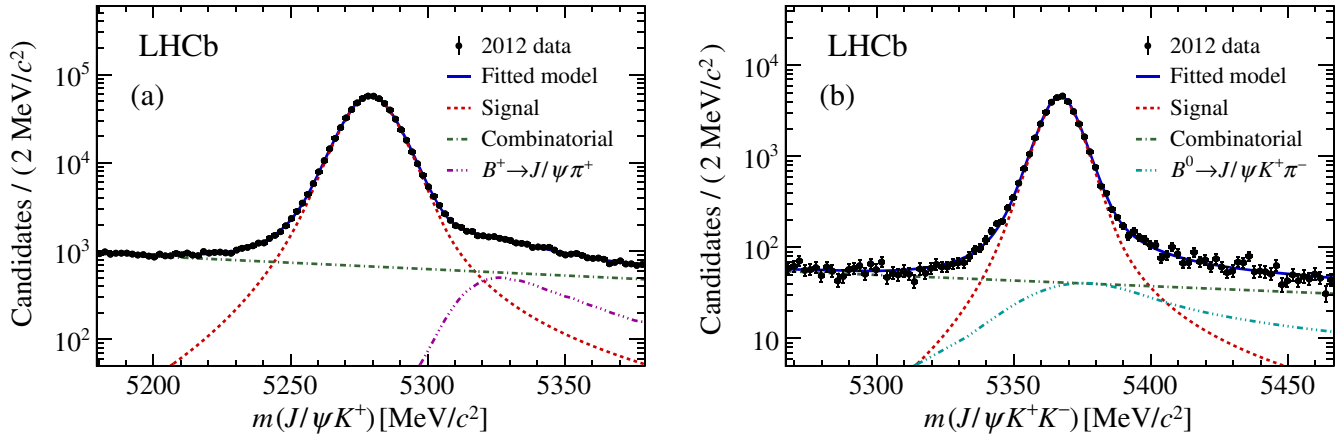

FIG. 1. Mass distributions of (a) $B^+ \to J/\psi K^+$ and (b) $B_s^0 \to J/\psi\phi$ candidates in the 2012 data. The result of the fit is drawn with a blue solid line. The model components are denoted with a red dashed line for the signal, green dot-dashed line for the combinatorial background, magenta triple-dot-dashed line for misidentified $B^+ \to J/\psi\pi^+$, and cyan triple-dot-dashed line for the misidentified inclusive $B^0 \to J/\psi K^+\pi^-$ contribution.

applied to simulated events. Its fraction, relative to the signal contribution, is found to be in agreement with the estimated fraction of $(3.8 \pm 0.1)\%$.

The dominant misidentified background in the $m(J/\psi K^+K^-)$ distribution arises from $B^0 \to J/\psi K^+\pi^-$ decays, where a pion is mistakenly reconstructed as a kaon. The total inclusive $B^0 \to J/\psi K^+\pi^-$ background is a combination of the resonant and nonresonant contributions in the $K^+\pi^-$ final state: $B^0 \to J/\psi K^*(892)^0$ and $B^0 \to J/\psi K^+\pi^-$. The PDFs of these components are linked [30], each described by a combination of two Crystal Ball functions [31] with a common Gaussian mean and tails on opposite sides. The background component is included in the fit model with the yield fraction defined relative to the signal contribution and the Gaussian constrained to the expected value of $(4.1 \pm 0.5)\%$, determined on simulation. Contributions from the decays $B_c^+ \to J/\psi K^+K^-\pi^+$, $B_s^0 \to J/\psi \bar{K}^{*0}$, $\Lambda_b^0 \to J/\psi pK^-$, $B_s^0 \to J/\psi\phi(\to K_S^0 K_L^0)$, and $B_s^0 \to J/\psi f_0(\to \pi^+\pi^-)$ are considered and found negligible. The fit results to the $B^+ \to J/\psi K^+$ and $B_s^0 \to J/\psi\phi$ candidates in 2012 data are shown in Fig. 1. Fits to all the samples are shown in the Supplemental Material [32].

The signal detection efficiencies include the detector acceptance, reconstruction efficiencies, and selection efficiencies. The efficiencies are computed using simulated samples unless stated otherwise. Tracking efficiency differences in data and simulation are corrected for. The corrections are applied for each final-state track separately, in bins of the track p_T and η and event multiplicity [33].

Trigger efficiencies are determined on data, separately for each data sample [34]. The trigger decision in every event can be ascribed to the reconstructed signal candidate and/or the rest of the event. The trigger efficiency is measured through the overlap of the two categories [35]. The abundant $B^+ \to J/\psi K^+$ sample is used to build a two-dimensional trigger efficiency map as a function of the p_T and p_L of the J/ψ candidates. The choice of variables accounts for small differences in the J/ψ kinematic distributions from $B^+ \to J/\psi K^+$ and $B_s^0 \to J/\psi\phi$ decays. The average signal trigger efficiencies are computed by weighting the map contents with the fractions of simulated events in each bin and averaging the results, separately for each signal mode. In case of the results in B-meson kinematic bins, the trigger efficiency maps are defined in bins of the considered kinematic variable and of an independent variable: p_T of the J/ψ candidate for the f_s/f_u results as a function of η^B, p_L^B, and y^B, and the p_L of the J/ψ candidate for results as a function of p_T^B.

Identical trigger selection and near-identical reconstruction and off-line selection significantly reduce the uncertainties affecting the efficiency-corrected $B_s^0 \to J/\psi\phi$ and $B^+ \to J/\psi K^+$ yield ratio measurement. Because of the similarity of J/ψ kinematic distributions from $B^+ \to J/\psi K^+$ and $B_s^0 \to J/\psi\phi$ decays, the efficiency ratios are close to unity, being about 0.98 for acceptance and selection and 0.99 for the trigger. The systematic uncertainties associated with acceptance, reconstruction, and selection efficiency arise only from the limited size of simulated samples. The dominant systematic uncertainties arise from the track-reconstruction efficiency corrections and the fit. A systematic uncertainty of 0.4% (0.8%) is assigned, following the procedures in Ref. [36], to the extra kaon track in $B_s^0 \to J/\psi\phi$ decays in 2011 and 2012 (2015 and 2016) samples. For all the samples, the uncertainty is increased by an additional 1.1% due to the interactions between the hadrons and detector material [36].

The systematic uncertainty arising from the fit model is propagated to the fitted signal yields by allowing the parameters to float within Gaussian constraints with mean

TABLE I. Efficiency-corrected $B_s^0 \to J/\psi\phi$ and $B^+ \to J/\psi K^+$ yield ratios ($\mathcal{R}$) and uncertainties ($\sigma_{\rm tot}$), including the statistical uncertainty ($\sigma_{\rm stat}$) and the fully correlated and uncorrelated systematic uncertainties among the samples ($\sigma_{\rm syst}^{\rm uncor}$, $\sigma_{\rm syst}^{\rm cor}$). Individual contributions from tracking efficiency ($\sigma_{\rm syst}^{\rm track}$), acceptance, reconstruction, and selection efficiency ($\sigma_{\rm syst}^{\rm sel}$) and fit model ($\sigma_{\rm syst}^{\rm fit}$) are shown separately. Correlations stem from the common tracking and fit model uncertainties.

Year	$\sqrt{s}$ (TeV)	$\mathcal{R}$	$\sigma_{\rm tot}$	$\sigma_{\rm stat}$	$\sigma_{\rm syst}^{\rm uncor}$	$\sigma_{\rm syst}^{\rm cor}$	$\sigma_{\rm syst}^{\rm track}$	$\sigma_{\rm syst}^{\rm sel}$	$\sigma_{\rm syst}^{\rm fit}$
2011	7	0.1238	0.0024	0.0010	0.0018	0.0012	0.0015	0.0008	0.0013
2012	8	0.1270	0.0023	0.0007	0.0019	0.0012	0.0016	0.0005	0.0015
2015	13	0.1338	0.0030	0.0017	0.0022	0.0012	0.0019	0.0004	0.0016
2016	13	0.1319	0.0024	0.0008	0.0021	0.0007	0.0018	0.0004	0.0012

and width determined from the simulation. Most of the signal and misidentified background component shape parameters are constrained with the remaining (partially correlated) tail parameters fixed to the values determined from simulation. The effect of fixing or leaving the signal parameters free has a negligible effect on the yield.

The resonant and nonresonant structure of the $m(J/\psi K^+K^-)$ spectrum is measured in Ref. [37]. The resonant $f_0(980)$ meson contribution, nonresonant S-wave contribution, and the interference effects are studied on simulated samples. No attempt is made to separate these contributions from the signal decays, and the uncertainty of the fitted inclusive $B_s^0 \to J/\psi\phi$ yield is increased by 0.8%, relative to the yield.

The fit models are validated using the fitted PDFs to generate and fit a large number of simulated pseudoexperiments according to the observed candidate yields. The pseudoexperiments are generated for the fits on the full samples as well as for the fits in bins of p_T^B and η^B. The mass fits in the p_T^B and η^B bins do not show a significant bias and no additional systematic uncertainty is included. The pseudoexperiments for the full samples show a small yield estimator bias, the largest of which is 20% of the statistical uncertainty. The uncertainties on these yields are therefore increased by the same amount to account for this.

The validity of the mass models over the B-meson phase space is verified by comparing the fitted fractions and the model parameters across the samples and bins. The $B^+ \to J/\psi K^+$ fit is performed with the $B^+ \to J/\psi\pi^+$ background shape determined independently in high- and low-p_T^B regions of the simulated decays. The variation in the observed yield is negligible. The background shapes in regions of η^B are very similar. The misidentified $B^0 \to J/\psi K^+\pi^-$ background PDF variation in p_T^B or η^B regions is studied with simulation. The distributions show no evidence for significant variation and no additional uncertainty is assigned to the fits in bins due to the assumption of the same fit model.

The ratios ($\mathcal{R}$) and their detailed uncertainty composition are shown in Table I. The ratios are fitted as a function of the pp collision energy with a two-parameter function: $a + k_s\sqrt{s}$, as shown in Fig. 2. The statistical significance of the f_s/f_u dependence on collision energy is estimated by comparing this fit with that under the null hypothesis $k_s = 0$. The χ^2 difference between the two cases is used as a test statistic and its p value is determined from the χ^2 distribution with one degree of freedom [38]. The two-sided significance of the two-parameter fit ($a = 0.1159 \pm 0.0032$, $k_s = (1.27 \pm 0.27) \times 10^{-3}$ TeV^{-1}, correlation $\rho = -0.76$) is 4.8σ with respect to the hypothesis of no energy dependence. The fit accounts for the correlations between the samples due to the common tracking and fit uncertainties as described in Ref. [32].

The measured double ratios for different collision energies are

$$\mathcal{R}_{8\ \rm TeV}/\mathcal{R}_{7\ \rm TeV} = 1.026 \pm 0.017,$$
$$\mathcal{R}_{13\ \rm TeV}/\mathcal{R}_{7\ \rm TeV} = 1.068 \pm 0.016,$$

with the correlation coefficient $\rho = 0.33$ between the two and the correlated uncertainties accounted for.

In each sample, the efficiency-corrected signal yield ratios are measured in bins of the B-meson kinematic variables $v \in \{p^B, p_T^B, p_L^B, \eta^B, y^B\}$ and averaged. On the vertical scale of Fig. 3, the averaged signal-yield ratios are scaled, assuming $f_u = f_d$, to match the average f_s/f_d

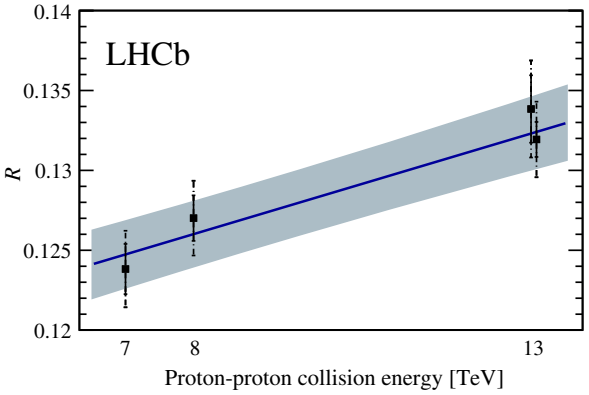

FIG. 2. Efficiency-corrected $B_s^0 \to J/\psi\phi$ and $B^+ \to J/\psi K^+$ yield ratios ($\mathcal{R}$) at different pp collision energies with the total (uncorrelated, including statistical) uncertainties denoted by dashed (solid) error bars. The fit result is shown with the blue solid line; the blue band denotes the 68% confidence region. The 13 TeV measurements are shifted horizontally for clarity.

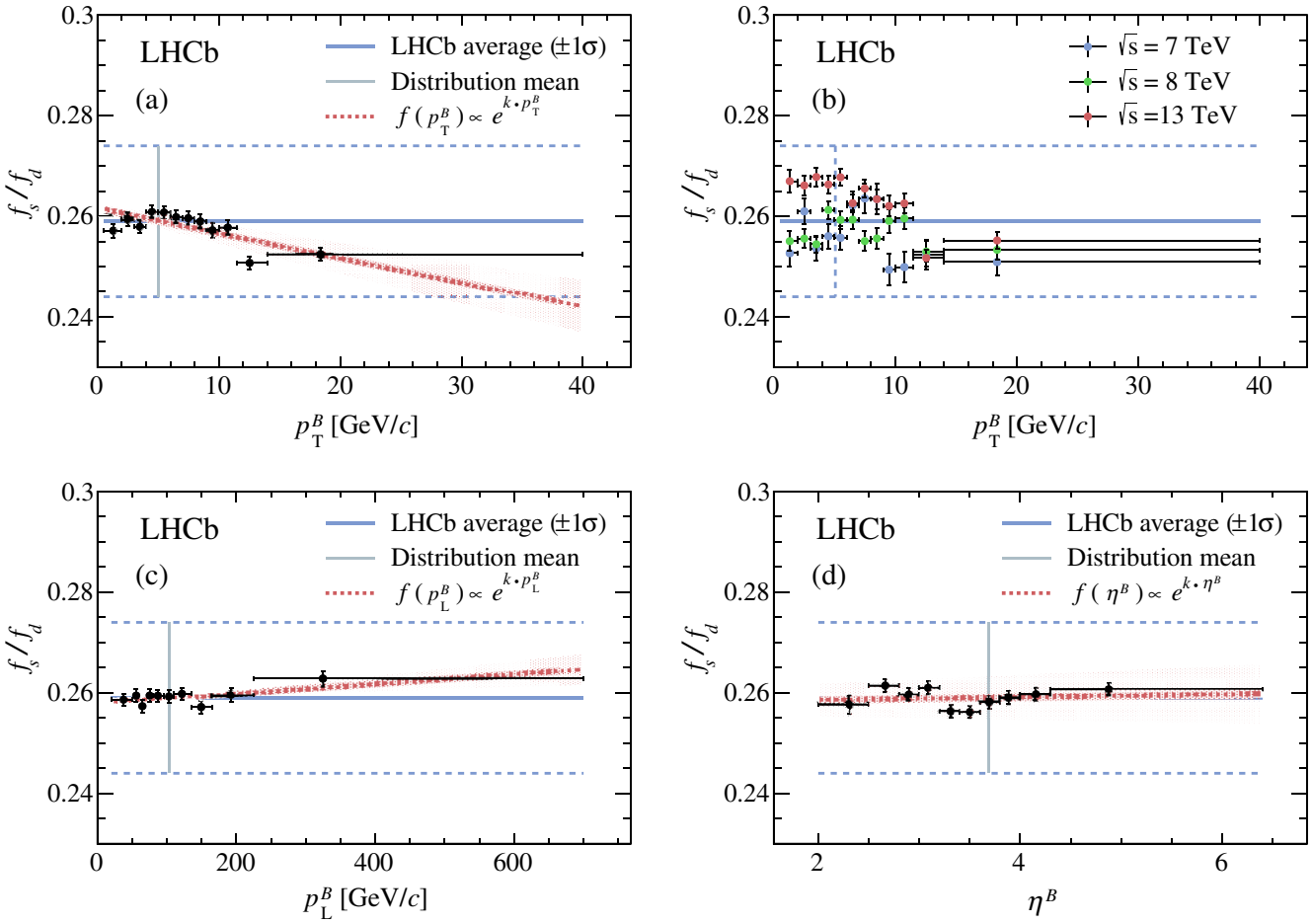

FIG. 3. Efficiency-corrected $B_s^0 \to J/\psi\phi$ and $B^+ \to J/\psi K^+$ yield ratios ($\mathcal{R}$) in bins of (a) p_T^B, (c) p_L^B, and (d) η^B. The ratios are scaled to match the measured f_s/f_d value (horizontal blue lines; the $\pm 1\sigma$ interval is indicated by the dashed blue lines) at the positions indicated by the vertical gray lines. The red dashed lines denote the results of the exponential fits used to estimate the statistical significances of the variations (see text). (b) The results as a function of p_T^B are obtained separately in the three collision energies.

value measured at $\sqrt{s} = 7$ TeV ($f_s/f_d = 0.259$) [10,39,40] at the corresponding variable distribution means; this is for illustrative purpose alone. On the horizontal scale, each data point is set to the mean value determined from simulation. The statistical significance of the f_s/f_u dependence is estimated by fitting the $\mathcal{R}$ distributions with a function $A_v \exp(k_v v)$ under two hypotheses: one where no variation is allowed and the slope parameter k_v is fixed to zero and one with k_v left free.

The relative B_s^0 and B^+ production is observed to depend on the p_T^B with a significance of 6σ and the fitted slope parameter is $k_{p_T^B} = -(1.93 \pm 0.46) \times 10^{-3}$ GeV^{-1}c. The strongest variation is measured for the 13 TeV samples: 8.7σ, $k_{p_T^B} = -(4.40 \pm 0.67) \times 10^{-3}$ GeV^{-1}c, while it is not significant (2.1σ and 1.5σ) for the 7 and 8 TeV results obtained separately; see the Supplemental Material [32] for further details. The variation in p_T^B is further studied in three subregions of p_L^B ($[20, 75, 125, 700]$ GeV/c) and a clear dependence is seen in all the regions. The results for p_T^B, p_L^B, and η^B are shown in Fig. 3. No evidence is found for significant f_s/f_u variation in p^B, p_L^B, η^B, or y^B. For the numerical results in all the studied variables and additional figures, see the Supplemental Material [32].

In conclusion, the B_s^0 and B^+ fragmentation-fraction ratio f_s/f_u is studied at 7, 8, and 13 TeV pp collision energies and in different B-meson kinematic regions. A 4.8σ evidence is seen for a f_s/f_u dependence on the collision energy and f_s/f_u is observed to depend on the B-meson transverse momentum. The observed p_T^B dependence is compatible with the recent LHCb result on semileptonic modes [9]. No evidence of f_s/f_u variation is seen in B-meson momentum, longitudinal momentum, rapidity, or pseudorapidity.

We express our gratitude to our colleagues in the CERN accelerator departments for the excellent performance of the LHC. We thank the technical and administrative staff at the LHCb institutes. We acknowledge support from CERN and from the national agencies: CAPES, CNPq, FAPERJ, and FINEP (Brazil), MOST and NSFC (China), CNRS/IN2P3 (France); BMBF, DFG, and MPG (Germany), INFN

(Italy), NWO (Netherlands), MNiSW and NCN (Poland), MEN/IFA (Romania), MSHE (Russia), MinECo (Spain), SNSF and SER (Switzerland), NASU (Ukraine), STFC (United Kingdom), and DOE NP and NSF (U.S.). We acknowledge the computing resources that are provided by CERN, IN2P3 (France), KIT and DESY (Germany), INFN (Italy), SURF (Netherlands), PIC (Spain), GridPP (United Kingdom), RRCKI and Yandex LLC (Russia), CSCS (Switzerland), IFIN-HH (Romania), CBPF (Brazil), PL-GRID (Poland), and OSC (U.S.). We are indebted to the communities behind the multiple open-source software packages on which we depend. Individual groups or members have received support from AvH Foundation (Germany), EPLANET, Marie Skłodowska-Curie Actions, and ERC (European Union), ANR, Labex P2IO, and OCEVU, and Région Auvergne-Rhône-Alpes (France), Key Research Program of Frontier Sciences of CAS, CAS PIFI, and the Thousand Talents Program (China), RFBR, RSF, and Yandex LLC (Russia), GVA, XuntaGal, and GENCAT (Spain), and the Royal Society and the Leverhulme Trust (United Kingdom).

[1] P. D. Acton *et al.* (OPAL Collaboration), Evidence for the existence of the strange b-flavoured meson B_s^0 in Z^0 decays, Phys. Lett. B **295**, 357 (1992).

[2] D. Buskulic *et al.* (ALEPH Collaboration), Measurement of the B_s^0 lifetime and production rate with $D_s^- \ell^+$ combinations in Z decays, Phys. Lett. B **361**, 221 (1995).

[3] M. Acciarri *et al.* (L3 Collaboration), Measurements of the $b\bar{b}$ production cross-section and forward-backward asymmetry at centre-of-mass energies above the Z pole at LEP, Phys. Lett. B **485**, 71 (2000).

[4] J. Abdallah *et al.* (DELPHI Collaboration), A Measurement of the branching fractions of the b quark into charged and neutral b hadrons, Phys. Lett. B **576**, 29 (2003).

[5] T. Aaltonen *et al.* (CDF Collaboration), Measurement of ratios of fragmentation fractions for bottom hadrons in $p\bar{p}$ collisions at $\sqrt{s} = 1.96$ TeV, Phys. Rev. D **77**, 072003 (2008).

[6] M. Tanabashi *et al.* (Particle Data Group), Review of particle physics, Phys. Rev. D **98**, 030001 (2018).

[7] T. Aaltonen *et al.* (CDF Collaboration), First measurement of the ratio of branching fractions $\mathcal{B}(\Lambda_b^0 \to \Lambda_c^+ \mu^- \bar{\nu}_\mu)/\mathcal{B}(\Lambda_b^0 \to \Lambda_c^+ \pi^-)$, Phys. Rev. D **79**, 032001 (2009).

[8] R. Aaij *et al.* (LHCb Collaboration), Study of the kinematic dependences of Λ_b^0 production in pp collisions and a measurement of the $\Lambda_b^0 \to \Lambda_c^+ \pi^-$ branching fraction, J. High Energy Phys. 08 (**2014**) 143.

[9] R. Aaij *et al.* (LHCb Collaboration), Measurement of b-hadron fractions in 13 TeV pp collisions, Phys. Rev. D **100**, 031102(R) (2019).

[10] R. Aaij *et al.* (LHCb Collaboration), Measurement of the fragmentation fraction ratio f_s/f_d and its dependence on B meson kinematics, J. High Energy Phys. 04 (2013) 001.

[11] V. Khachatryan *et al.* (CMS and LHCb Collaborations), Observation of the rare $B_s^0 \to \mu^+ \mu^-$ decay from the combined analysis of CMS and LHCb data, Nature (London) **522**, 68 (2015).

[12] R. Aaij *et al.* (LHCb Collaboration), Measurement of the $B_s^0 \to \mu^+ \mu^-$ Branching Fraction and Effective Lifetime and Search for $B^0 \to \mu^+ \mu^-$ Decays, Phys. Rev. Lett. **118**, 191801 (2017).

[13] G. Aad *et al.* (ATLAS Collaboration), Determination of the Ratio of b-Quark Fragmentation Fractions f_s/f_d in pp Collisions at $\sqrt{s} = 7$ TeV with the ATLAS Detector, Phys. Rev. Lett. **115**, 262001 (2015).

[14] X. Liu, W. Wang, and Y. Xie, Penguin pollution in $B \to J/\psi V$ decays and impact on the extraction of the $B_s - \bar{B}_s$ mixing phase, Phys. Rev. D **89**, 094010 (2014).

[15] J. Adam *et al.* (ALICE Collaboration), Enhanced production of multi-strange hadrons in high-multiplicity proton-proton collisions, Nat. Phys. **13**, 535 (2017).

[16] S. Acharya *et al.* (ALICE Collaboration), Multiplicity dependence of light-flavor hadron production in pp collisions at $\sqrt{s} = 7$ TeV, Phys. Rev. C **99**, 024906 (2019).

[17] S. Acharya *et al.* (ALICE Collaboration), Multiplicity dependence of (multi-)strange hadron production in proton-proton collisions at $\sqrt{s} = 13$ TeV, Eur. Phys. J. C **80**, 167 (2020).

[18] A. A. Alves *et al.* (LHCb Collaboration), The LHCb detector at the LHC, J. Instrum. **3**, S08005 (2008).

[19] R. Aaij *et al.* (LHCb Collaboration), LHCb detector performance, Int. J. Mod. Phys. A **30**, 1530022 (2015).

[20] F. Archilli *et al.*, Performance of the muon identification at LHCb, J. Instrum. **8**, P10020 (2013).

[21] T. Sjöstrand, S. Mrenna, and P. Skands, A brief introduction to PYTHIA8.1, Comput. Phys. Commun. **178**, 852 (2008).

[22] I. Belyaev *et al.*, Handling of the generation of primary events in Gauss, the LHCb simulation framework, J. Phys. Conf. Ser. **331**, 032047 (2011).

[23] D. J. Lange, The EvtGen particle decay simulation package, Nucl. Instrum. Methods Phys. Res., Sect. A **462**, 152 (2001).

[24] P. Golonka and Z. Was, PHOTOS Monte Carlo: A precision tool for QED corrections in Z and W decays, Eur. Phys. J. C **45**, 97 (2006).

[25] S. Agostinelli *et al.* (GEANT4 Collaboration), GEANT4: A simulation toolkit, Nucl. Instrum. Methods Phys. Res., Sect. A **506**, 250 (2003).

[26] M. Clemencic, G. Corti, S. Easo, C. R. Jones, S. Miglioranzi, M. Pappagallo, and P. Robbe, The LHCb simulation application, Gauss: Design, evolution and experience, J. Phys. Conf. Ser. **331**, 032023 (2011).

[27] R. Aaij *et al.* (LHCb Collaboration), Measurement of the $B^\pm$ production cross-section in pp collisions at $\sqrt{s} = 7$ and 13 TeV, J. High Energy Phys. 12 (2017) 026.

[28] D. Martínez Santos and F. Dupertuis, Mass distributions marginalized over per-event errors, Nucl. Instrum. Methods Phys. Res., Sect. A **764**, 150 (2014).

[29] K. S. Cranmer, Kernel estimation in high-energy physics, Comput. Phys. Commun. **136**, 198 (2001).

[30] K. Chilikin *et al.* (Belle Collaboration), Observation of a new charged charmoniumlike state in $\bar{B}^0 \to J/\psi K^- \pi^+$ decays, Phys. Rev. D **90**, 112009 (2014).

[31] T. Skwarnicki, A study of the radiative CASCADE transitions between the Upsilon-Prime and Upsilon resonances, Ph.D. thesis, Institute of Nuclear Physics, Krakow, 1986, http://inspirehep.net/record/230779.
[32] See Supplemental Material at http://link.aps.org/supplemental/10.1103/PhysRevLett.124.122002 for additional plots and tables.
[33] R. Aaij *et al.* (LHCb Collaboration), Measurement of the track reconstruction efficiency at LHCb, J. Instrum. **10**, P02007 (2015).
[34] S. Tolk, J. Albrecht, F. Dettori, and A. Pellegrino, Data driven trigger efficiency determination at LHCb, Technical Reports No. LHCb-PUB-2014-039, CERN-LHCb-PUB-2014-039, CERN, Geneva, 2014, https://cds.cern.ch/record/1701134.
[35] R. Aaij *et al.*, The LHCb trigger and its performance in 2011, J. Instrum. **8**, P04022 (2013).
[36] R. Aaij *et al.* (LHCb Collaboration), Measurement of the track reconstruction efficiency at LHCb, J. Instrum. **10**, P02007 (2015).
[37] R. Aaij *et al.* (LHCb Collaboration), Amplitude analysis and branching fraction measurement of $\bar{B}^0_s \to J/\psi K^+K^-$, Phys. Rev. D **87**, 072004 (2013).
[38] S. S. Wilks, The large-sample distribution of the likelihood ratio for testing composite hypotheses, Ann. Math. Stat. **9**, 60 (1938).
[39] R. Aaij *et al.* (LHCb Collaboration), Measurement of b hadron production fractions in 7 TeV pp collisions, Phys. Rev. D **85**, 032008 (2012).
[40] LHCb Collaboration, Updated average f_s/f_d b-hadron production fraction ratio for 7 TeV pp collisions, Report No. LHCb-CONF-2013-011, 2013, https://cds.cern.ch/record/1559262.

R. Aaij,[30] C. Abellán Beteta,[47] B. Adeva,[44] M. Adinolfi,[51] C. A. Aidala,[78] Z. Ajaltouni,[8] S. Akar,[62] P. Albicocco,[21] J. Albrecht,[13] F. Alessio,[45] M. Alexander,[56] A. Alfonso Albero,[43] G. Alkhazov,[36] P. Alvarez Cartelle,[58] A. A. Alves Jr.,[44] S. Amato,[2] Y. Amhis,[10] L. An,[20] L. Anderlini,[20] G. Andreassi,[46] M. Andreotti,[19] J. E. Andrews,[63] F. Archilli,[21] J. Arnau Romeu,[9] A. Artamonov,[42] M. Artuso,[65] K. Arzymatov,[40] E. Aslanides,[9] M. Atzeni,[47] B. Audurier,[25] S. Bachmann,[15] J. J. Back,[53] S. Baker,[58] V. Balagura,[10,b] W. Baldini,[19,45] A. Baranov,[40] R. J. Barlow,[59] S. Barsuk,[10] W. Barter,[58] M. Bartolini,[22,c] F. Baryshnikov,[74] V. Batozskaya,[34] B. Batsukh,[65] A. Battig,[13] V. Battista,[46] A. Bay,[46] F. Bedeschi,[27] I. Bediaga,[1] A. Beiter,[65] L. J. Bel,[30] V. Belavin,[40] S. Belin,[25] N. Beliy,[4] V. Bellee,[46] K. Belous,[42] I. Belyaev,[37] G. Bencivenni,[21] E. Ben-Haim,[11] S. Benson,[30] S. Beranek,[12] A. Berezhnoy,[38] R. Bernet,[47] D. Berninghoff,[15] H. C. Bernstein,[65] E. Bertholet,[11] A. Bertolin,[26] C. Betancourt,[47] F. Betti,[18,d] M. O. Bettler,[52] Ia. Bezshyiko,[47] S. Bhasin,[51] J. Bhom,[32] M. S. Bieker,[13] S. Bifani,[50] P. Billoir,[11] A. Birnkraut,[13] A. Bizzeti,[20,e] M. Bjørn,[60] M. P. Blago,[45] T. Blake,[53] F. Blanc,[46] S. Blusk,[65] D. Bobulska,[56] V. Bocci,[29] O. Boente Garcia,[44] T. Boettcher,[61] A. Boldyrev,[75] A. Bondar,[41,f] N. Bondar,[36] S. Borghi,[59,45] M. Borisyak,[40] M. Borsato,[15] M. Boubdir,[12] T. J. V. Bowcock,[57] C. Bozzi,[19,45] S. Braun,[15] A. Brea Rodriguez,[44] M. Brodski,[45] J. Brodzicka,[32] A. Brossa Gonzalo,[53] D. Brundu,[25,45] E. Buchanan,[51] A. Buonaura,[47] C. Burr,[59] A. Bursche,[25] J. S. Butter,[30] J. Buytaert,[45] W. Byczynski,[45] S. Cadeddu,[25] H. Cai,[69] R. Calabrese,[19,g] S. Cali,[21] R. Calladine,[50] M. Calvi,[23,h] M. Calvo Gomez,[43,i] A. Camboni,[43,i] P. Campana,[21] D. H. Campora Perez,[45] L. Capriotti,[18,d] A. Carbone,[18,d] G. Carboni,[28] R. Cardinale,[22,c] A. Cardini,[25] P. Carniti,[23,h] K. Carvalho Akiba,[30] A. Casais Vidal,[44] G. Casse,[57] M. Cattaneo,[45] G. Cavallero,[22] R. Cenci,[27,j] M. G. Chapman,[51] M. Charles,[11,45] Ph. Charpentier,[45] G. Chatzikonstantinidis,[50] M. Chefdeville,[7] V. Chekalina,[40] C. Chen,[3] S. Chen,[25] S.-G. Chitic,[45] V. Chobanova,[44] M. Chrzaszcz,[45] A. Chubykin,[36] P. Ciambrone,[21] X. Cid Vidal,[44] G. Ciezarek,[45] F. Cindolo,[18] P. E. L. Clarke,[55] M. Clemencic,[45] H. V. Cliff,[52] J. Closier,[45] J. L. Cobbledick,[59] V. Coco,[45] J. A. B. Coelho,[10] J. Cogan,[9] E. Cogneras,[8] L. Cojocariu,[35] P. Collins,[45] T. Colombo,[45] A. Comerma-Montells,[15] A. Contu,[25] N. Cooke,[50] G. Coombs,[45] S. Coquereau,[43] G. Corti,[45] C. M. Costa Sobral,[53] B. Couturier,[45] G. A. Cowan,[55] D. C. Craik,[61] A. Crocombe,[53] M. Cruz Torres,[1] R. Currie,[55] C. L. Da Silva,[64] E. Dall'Occo,[30] J. Dalseno,[44,51] C. D'Ambrosio,[45] A. Danilina,[37] P. d'Argent,[15] A. Davis,[59] O. De Aguiar Francisco,[45] K. De Bruyn,[45] S. De Capua,[59] M. De Cian,[46] J. M. De Miranda,[1] L. De Paula,[2] M. De Serio,[17,k] P. De Simone,[21] J. A. de Vries,[30] C. T. Dean,[56] W. Dean,[78] D. Decamp,[7] L. Del Buono,[11] B. Delaney,[52] H.-P. Dembinski,[14] M. Demmer,[13] A. Dendek,[33] V. Denysenko,[47] D. Derkach,[75] O. Deschamps,[8] F. Desse,[10] F. Dettori,[25,r] B. Dey,[6] A. Di Canto,[45] P. Di Nezza,[21] S. Didenko,[74] H. Dijkstra,[45] F. Dordei,[25] M. Dorigo,[27,l] A. C. dos Reis,[1] A. Dosil Suárez,[44] L. Douglas,[56] A. Dovbnya,[48] K. Dreimanis,[57] L. Dufour,[45] G. Dujany,[11] P. Durante,[45] J. M. Durham,[64] D. Dutta,[59] R. Dzhelyadin,[42,a] M. Dziewiecki,[15] A. Dziurda,[32] A. Dzyuba,[36] S. Easo,[54] U. Egede,[58] V. Egorychev,[37] S. Eidelman,[41,f] S. Eisenhardt,[55] U. Eitschberger,[13] R. Ekelhof,[13] S. Ek-In,[46] L. Eklund,[56] S. Ely,[65] A. Ene,[35] S. Escher,[12] S. Esen,[30] T. Evans,[62] A. Falabella,[18] C. Färber,[45] N. Farley,[50] S. Farry,[57] D. Fazzini,[10] M. Féo,[45] P. Fernandez Declara,[45] A. Fernandez Prieto,[44] F. Ferrari,[18,d] L. Ferreira Lopes,[46] F. Ferreira Rodrigues,[2] S. Ferreres Sole,[30] M. Ferro-Luzzi,[45] S. Filippov,[39] R. A. Fini,[17] M. Fiorini,[19,g] M. Firlej,[33] C. Fitzpatrick,[45] T. Fiutowski,[33] F. Fleuret,[10,b] M. Fontana,[45]

F. Fontanelli,[22,c] R. Forty,[45] V. Franco Lima,[57] M. Franco Sevilla,[63] M. Frank,[45] C. Frei,[45] J. Fu,[24,m] W. Funk,[45] E. Gabriel,[55] A. Gallas Torreira,[44] D. Galli,[18,d] S. Gallorini,[26] S. Gambetta,[55] Y. Gan,[3] M. Gandelman,[2] P. Gandini,[24] Y. Gao,[3] L. M. Garcia Martin,[77] J. García Pardiñas,[47] B. Garcia Plana,[44] J. Garra Tico,[52] L. Garrido,[43] D. Gascon,[43] C. Gaspar,[45] G. Gazzoni,[8] D. Gerick,[15] E. Gersabeck,[59] M. Gersabeck,[59] T. Gershon,[53] D. Gerstel,[9] Ph. Ghez,[7] V. Gibson,[52] A. Gioventù,[44] O. G. Girard,[46] P. Gironella Gironell,[43] L. Giubega,[35] K. Gizdov,[55] V. V. Gligorov,[11] C. Göbel,[67] D. Golubkov,[37] A. Golutvin,[58,74] A. Gomes,[1,n] I. V. Gorelov,[38] C. Gotti,[23,h] E. Govorkova,[30] J. P. Grabowski,[15] R. Graciani Diaz,[43] L. A. Granado Cardoso,[45] E. Graugés,[43] E. Graverini,[46] G. Graziani,[20] A. Grecu,[35] R. Greim,[30] P. Griffith,[25] L. Grillo,[59] L. Gruber,[45] B. R. Gruberg Cazon,[60] C. Gu,[3] E. Gushchin,[39] A. Guth,[12] Yu. Guz,[42,45] T. Gys,[45] T. Hadavizadeh,[60] C. Hadjivasiliou,[8] G. Haefeli,[46] C. Haen,[45] S. C. Haines,[52] P. M. Hamilton,[63] Q. Han,[6] X. Han,[15] T. H. Hancock,[60] S. Hansmann-Menzemer,[15] N. Harnew,[60] T. Harrison,[57] C. Hasse,[45] M. Hatch,[45] J. He,[4] M. Hecker,[58] K. Heijhoff,[30] K. Heinicke,[13] A. Heister,[13] K. Hennessy,[57] L. Henry,[77] M. Heß,[71] J. Heuel,[12] A. Hicheur,[66] R. Hidalgo Charman,[59] D. Hill,[60] M. Hilton,[59] P. H. Hopchev,[46] J. Hu,[15] W. Hu,[6] W. Huang,[4] Z. C. Huard,[62] W. Hulsbergen,[30] T. Humair,[58] M. Hushchyn,[75] D. Hutchcroft,[57] D. Hynds,[30] P. Ibis,[13] M. Idzik,[33] P. Ilten,[50] A. Inglessi,[36] A. Inyakin,[42] K. Ivshin,[36] R. Jacobsson,[45] S. Jakobsen,[45] J. Jalocha,[60] E. Jans,[30] B. K. Jashal,[77] A. Jawahery,[63] F. Jiang,[3] M. John,[60] D. Johnson,[45] C. R. Jones,[52] C. Joram,[45] B. Jost,[45] N. Jurik,[60] S. Kandybei,[48] M. Karacson,[45] J. M. Kariuki,[51] S. Karodia,[56] N. Kazeev,[75] M. Kecke,[15] F. Keizer,[52] M. Kelsey,[65] M. Kenzie,[52] T. Ketel,[31] B. Khanji,[45] A. Kharisova,[76] C. Khurewathanakul,[46] K. E. Kim,[65] T. Kirn,[12] V. S. Kirsebom,[46] S. Klaver,[21] K. Klimaszewski,[34] S. Koliiev,[49] M. Kolpin,[15] A. Kondybayeva,[74] A. Konoplyannikov,[37] P. Kopciewicz,[33] R. Kopecna,[15] P. Koppenburg,[30] I. Kostiuk,[30,49] O. Kot,[49] S. Kotriakhova,[36] M. Kozeiha,[8] L. Kravchuk,[39] M. Kreps,[53] F. Kress,[58] S. Kretzschmar,[12] P. Krokovny,[41,f] W. Krupa,[33] W. Krzemien,[34] W. Kucewicz,[32,o] M. Kucharczyk,[32] V. Kudryavtsev,[41,f] G. J. Kunde,[64] A. K. Kuonen,[46] T. Kvaratskheliya,[37] D. Lacarrere,[45] G. Lafferty,[59] A. Lai,[25] D. Lancierini,[47] J. J. Lane,[59] G. Lanfranchi,[21] C. Langenbruch,[12] T. Latham,[53] C. Lazzeroni,[50] R. Le Gac,[9] R. Lefèvre,[8] A. Leflat,[38] F. Lemaitre,[45] O. Leroy,[9] T. Lesiak,[32] B. Leverington,[15] H. Li,[68] P.-R. Li,[4,p] X. Li,[64] Y. Li,[5] Z. Li,[65] X. Liang,[65] T. Likhomanenko,[73] R. Lindner,[45] F. Lionetto,[47] V. Lisovskyi,[10] G. Liu,[68] X. Liu,[3] D. Loh,[53] A. Loi,[25] J. Lomba Castro,[44] I. Longstaff,[56] J. H. Lopes,[2] G. Loustau,[47] G. H. Lovell,[52] D. Lucchesi,[26,q] M. Lucio Martinez,[44] Y. Luo,[3] A. Lupato,[26] E. Luppi,[19,g] O. Lupton,[53] A. Lusiani,[27] X. Lyu,[4] F. Machefert,[10] F. Maciuc,[35] V. Macko,[46] P. Mackowiak,[13] S. Maddrell-Mander,[51] O. Maev,[36,45] A. Maevskiy,[75] K. Maguire,[59] D. Maisuzenko,[36] M. W. Majewski,[33] S. Malde,[60] B. Malecki,[45] A. Malinin,[73] T. Maltsev,[41,f] H. Malygina,[15] G. Manca,[25,r] G. Mancinelli,[9] D. Marangotto,[24,m] J. Maratas,[8,s] J. F. Marchand,[7] U. Marconi,[18] C. Marin Benito,[10] M. Marinangeli,[46] P. Marino,[46] J. Marks,[15] P. J. Marshall,[57] G. Martellotti,[29] L. Martinazzoli,[45] M. Martinelli,[45,23,h] D. Martinez Santos,[44] F. Martinez Vidal,[77] A. Massafferri,[1] M. Materok,[12] R. Matev,[45] A. Mathad,[47] Z. Mathe,[45] V. Matiunin,[37] C. Matteuzzi,[23] K. R. Mattioli,[78] A. Mauri,[47] E. Maurice,[10,b] B. Maurin,[46] M. McCann,[58,45] L. Mcconnell,[16] A. McNab,[59] R. McNulty,[16] J. V. Mead,[57] B. Meadows,[62] C. Meaux,[9] N. Meinert,[71] D. Melnychuk,[34] M. Merk,[30] A. Merli,[24,m] E. Michielin,[26] D. A. Milanes,[70] E. Millard,[53] M.-N. Minard,[7] O. Mineev,[37] L. Minzoni,[19,g] D. S. Mitzel,[15] A. Mödden,[13] A. Mogini,[11] R. D. Moise,[58] T. Mombächer,[13] I. A. Monroy,[70] S. Monteil,[8] M. Morandin,[26] G. Morello,[21] M. J. Morello,[27,t] J. Moron,[33] A. B. Morris,[9] R. Mountain,[65] H. Mu,[3] F. Muheim,[55] M. Mukherjee,[6] M. Mulder,[30] D. Müller,[45] J. Müller,[13] K. Müller,[47] V. Müller,[13] C. H. Murphy,[60] D. Murray,[59] P. Naik,[51] T. Nakada,[46] R. Nandakumar,[54] A. Nandi,[60] T. Nanut,[46] I. Nasteva,[2] M. Needham,[55] N. Neri,[24,m] S. Neubert,[15] N. Neufeld,[45] R. Newcombe,[58] T. D. Nguyen,[46] C. Nguyen-Mau,[46,u] S. Nieswand,[12] R. Niet,[13] N. Nikitin,[38] N. S. Nolte,[45] A. Oblakowska-Mucha,[33] V. Obraztsov,[42] S. Ogilvy,[56] D. P. O'Hanlon,[18] R. Oldeman,[25,r] C. J. G. Onderwater,[72] J. D. Osborn,[78] A. Ossowska,[32] J. M. Otalora Goicochea,[2] T. Ovsiannikova,[37] P. Owen,[47] A. Oyanguren,[77] P. R. Pais,[46] T. Pajero,[27,t] A. Palano,[17] M. Palutan,[21] G. Panshin,[76] A. Papanestis,[54] M. Pappagallo,[55] L. L. Pappalardo,[19,g] W. Parker,[63] C. Parkes,[59,45] G. Passaleva,[20,45] A. Pastore,[17] M. Patel,[58] C. Patrignani,[18,d] A. Pearce,[45] A. Pellegrino,[30] G. Penso,[29] M. Pepe Altarelli,[45] S. Perazzini,[18] D. Pereima,[37] P. Perret,[8] L. Pescatore,[46] K. Petridis,[51] A. Petrolini,[22,c] A. Petrov,[73] S. Petrucci,[55] M. Petruzzo,[24,m] B. Pietrzyk,[7] G. Pietrzyk,[46] M. Pikies,[32] M. Pili,[60] D. Pinci,[29] J. Pinzino,[45] F. Pisani,[45] A. Piucci,[15] V. Placinta,[35] S. Playfer,[55] J. Plews,[50] M. Plo Casasus,[44] F. Polci,[11] M. Poli Lener,[21] M. Poliakova,[65] A. Poluektov,[9] N. Polukhina,[74,v] I. Polyakov,[65] E. Polycarpo,[2] G. J. Pomery,[51] S. Ponce,[45] A. Popov,[42] D. Popov,[50] S. Poslavskii,[42] K. Prasanth,[32] E. Price,[51] C. Prouve,[44] V. Pugatch,[49] A. Puig Navarro,[47] H. Pullen,[60] G. Punzi,[27,j] W. Qian,[4] J. Qin,[4] R. Quagliani,[11] B. Quintana,[8] N. V. Raab,[16] B. Rachwal,[33] J. H. Rademacker,[51] M. Rama,[27] M. Ramos Pernas,[44] M. S. Rangel,[2] F. Ratnikov,[40,75] G. Raven,[31] M. Ravonel Salzgeber,[45] M. Reboud,[7] F. Redi,[46] S. Reichert,[13] F. Reiss,[11] C. Remon Alepuz,[77] Z. Ren,[3] V. Renaudin,[60] S. Ricciardi,[54] S. Richards,[51]

K. Rinnert,[57] P. Robbe,[10] A. Robert,[11] A. B. Rodrigues,[46] E. Rodrigues,[62] J. A. Rodriguez Lopez,[70] M. Roehrken,[45] S. Roiser,[45] A. Rollings,[60] V. Romanovskiy,[42] A. Romero Vidal,[44] J. D. Roth,[78] M. Rotondo,[21] M. S. Rudolph,[65] T. Ruf,[45] J. Ruiz Vidal,[77] J. J. Saborido Silva,[44] N. Sagidova,[36] B. Saitta,[25,r] V. Salustino Guimaraes,[67] C. Sanchez Gras,[30] C. Sanchez Mayordomo,[77] B. Sanmartin Sedes,[44] R. Santacesaria,[29] C. Santamarina Rios,[44] M. Santimaria,[21,45] E. Santovetti,[28,w] G. Sarpis,[59] A. Sarti,[21,x] C. Satriano,[29,y] A. Satta,[28] M. Saur,[4] D. Savrina,[37,38] S. Schael,[12] M. Schellenberg,[13] M. Schiller,[56] H. Schindler,[45] M. Schmelling,[14] T. Schmelzer,[13] B. Schmidt,[45] O. Schneider,[46] A. Schopper,[45] H. F. Schreiner,[62] M. Schubiger,[30] S. Schulte,[46] M. H. Schune,[10] R. Schwemmer,[45] B. Sciascia,[21] A. Sciubba,[29,x] A. Semennikov,[37] E. S. Sepulveda,[11] A. Sergi,[50,45] N. Serra,[47] J. Serrano,[9] L. Sestini,[26] A. Seuthe,[13] P. Seyfert,[45] M. Shapkin,[42] T. Shears,[57] L. Shekhtman,[41,f] V. Shevchenko,[73] E. Shmanin,[74] B. G. Siddi,[19] R. Silva Coutinho,[47] L. Silva de Oliveira,[2] G. Simi,[26,q] S. Simone,[17,k] I. Skiba,[19] N. Skidmore,[15] T. Skwarnicki,[65] M. W. Slater,[50] J. G. Smeaton,[52] E. Smith,[12] I. T. Smith,[55] M. Smith,[58] M. Soares,[18] L. Soares Lavra,[1] M. D. Sokoloff,[62] F. J. P. Soler,[56] B. Souza De Paula,[2] B. Spaan,[13] E. Spadaro Norella,[24,m] P. Spradlin,[56] F. Stagni,[45] M. Stahl,[15] S. Stahl,[45] P. Stefko,[46] S. Stefkova,[58] O. Steinkamp,[47] S. Stemmle,[15] O. Stenyakin,[42] M. Stepanova,[36] H. Stevens,[13] S. Stone,[65] S. Stracka,[27] M. E. Stramaglia,[46] M. Straticiuc,[35] U. Straumann,[47] S. Strokov,[76] J. Sun,[3] L. Sun,[69] Y. Sun,[63] K. Swientek,[33] A. Szabelski,[34] T. Szumlak,[33] M. Szymanski,[4] Z. Tang,[3] T. Tekampe,[13] G. Tellarini,[19] F. Teubert,[45] E. Thomas,[45] M. J. Tilley,[58] V. Tisserand,[8] S. T'Jampens,[7] M. Tobin,[5] S. Tolk,[45] L. Tomassetti,[19,g] D. Tonelli,[27] D. Y. Tou,[11] E. Tournefier,[7] M. Traill,[56] M. T. Tran,[46] A. Trisovic,[52] A. Tsaregorodtsev,[9] G. Tuci,[27,45,j] A. Tully,[52] N. Tuning,[30] A. Ukleja,[34] A. Usachov,[10] A. Ustyuzhanin,[40,75] U. Uwer,[15] A. Vagner,[76] V. Vagnoni,[18] A. Valassi,[45] S. Valat,[45] G. Valenti,[18] M. van Beuzekom,[30] H. Van Hecke,[64] E. van Herwijnen,[45] C. B. Van Hulse,[16] J. van Tilburg,[30] M. van Veghel,[30] R. Vazquez Gomez,[45] P. Vazquez Regueiro,[44] C. Vázquez Sierra,[30] S. Vecchi,[19] J. J. Velthuis,[51] M. Veltri,[20,z] A. Venkateswaran,[65] M. Vernet,[8] M. Veronesi,[30] M. Vesterinen,[53] J. V. Viana Barbosa,[45] D. Vieira,[4] M. Vieites Diaz,[44] H. Viemann,[71] X. Vilasis-Cardona,[43,i] A. Vitkovskiy,[30] M. Vitti,[52] V. Volkov,[38] A. Vollhardt,[47] D. Vom Bruch,[11] B. Voneki,[45] A. Vorobyev,[36] V. Vorobyev,[41,f] N. Voropaev,[36] R. Waldi,[71] J. Walsh,[27] J. Wang,[3] J. Wang,[5] M. Wang,[3] Y. Wang,[6] Z. Wang,[47] D. R. Ward,[52] H. M. Wark,[57] N. K. Watson,[50] D. Websdale,[58] A. Weiden,[47] C. Weisser,[61] D. J. White,[59] M. Whitehead,[12] G. Wilkinson,[60] M. Wilkinson,[65] I. Williams,[52] M. Williams,[61] M. R. J. Williams,[59] T. Williams,[50] F. F. Wilson,[54] M. Winn,[10] W. Wislicki,[34] M. Witek,[32] G. Wormser,[10] S. A. Wotton,[52] K. Wyllie,[45] Z. Xiang,[4] D. Xiao,[6] Y. Xie,[6] H. Xing,[68] A. Xu,[3] L. Xu,[3] M. Xu,[6] Q. Xu,[4] Z. Xu,[7] Z. Xu,[3] Z. Yang,[3] Z. Yang,[63] Y. Yao,[65] L. E. Yeomans,[57] H. Yin,[6] J. Yu,[6,aa] X. Yuan,[65] O. Yushchenko,[42] K. A. Zarebski,[50] M. Zavertyaev,[14,v] M. Zeng,[3] D. Zhang,[6] L. Zhang,[3] S. Zhang,[3] W. C. Zhang,[3,bb] Y. Zhang,[45] A. Zhelezov,[15] Y. Zheng,[4] X. Zhou,[4] Y. Zhou,[4] X. Zhu,[3] V. Zhukov,[12,38] J. B. Zonneveld,[55] and S. Zucchelli[18,d]

(LHCb Collaboration)

[1]*Centro Brasileiro de Pesquisas Físicas (CBPF), Rio de Janeiro, Brazil*
[2]*Universidade Federal do Rio de Janeiro (UFRJ), Rio de Janeiro, Brazil*
[3]*Center for High Energy Physics, Tsinghua University, Beijing, China*
[4]*University of Chinese Academy of Sciences, Beijing, China*
[5]*Institute Of High Energy Physics (IHEP), Beijing, China*
[6]*Institute of Particle Physics, Central China Normal University, Wuhan, Hubei, China*
[7]*Univ. Grenoble Alpes, Univ. Savoie Mont Blanc, CNRS, IN2P3-LAPP, Annecy, France*
[8]*Université Clermont Auvergne, CNRS/IN2P3, LPC, Clermont-Ferrand, France*
[9]*Aix Marseille Univ, CNRS/IN2P3, CPPM, Marseille, France*
[10]*LAL, Univ. Paris-Sud, CNRS/IN2P3, Université Paris-Saclay, Orsay, France*
[11]*LPNHE, Sorbonne Université, Paris Diderot Sorbonne Paris Cité, CNRS/IN2P3, Paris, France*
[12]*I. Physikalisches Institut, RWTH Aachen University, Aachen, Germany*
[13]*Fakultät Physik, Technische Universität Dortmund, Dortmund, Germany*
[14]*Max-Planck-Institut für Kernphysik (MPIK), Heidelberg, Germany*
[15]*Physikalisches Institut, Ruprecht-Karls-Universität Heidelberg, Heidelberg, Germany*
[16]*School of Physics, University College Dublin, Dublin, Ireland*
[17]*INFN Sezione di Bari, Bari, Italy*
[18]*INFN Sezione di Bologna, Bologna, Italy*
[19]*INFN Sezione di Ferrara, Ferrara, Italy*
[20]*INFN Sezione di Firenze, Firenze, Italy*

[21]INFN Laboratori Nazionali di Frascati, Frascati, Italy
[22]INFN Sezione di Genova, Genova, Italy
[23]INFN Sezione di Milano-Bicocca, Milano, Italy
[24]INFN Sezione di Milano, Milano, Italy
[25]INFN Sezione di Cagliari, Monserrato, Italy
[26]INFN Sezione di Padova, Padova, Italy
[27]INFN Sezione di Pisa, Pisa, Italy
[28]INFN Sezione di Roma Tor Vergata, Roma, Italy
[29]INFN Sezione di Roma La Sapienza, Roma, Italy
[30]Nikhef National Institute for Subatomic Physics, Amsterdam, Netherlands
[31]Nikhef National Institute for Subatomic Physics and VU University Amsterdam, Amsterdam, Netherlands
[32]Henryk Niewodniczanski Institute of Nuclear Physics Polish Academy of Sciences, Kraków, Poland
[33]AGH—University of Science and Technology, Faculty of Physics and Applied Computer Science, Kraków, Poland
[34]National Center for Nuclear Research (NCBJ), Warsaw, Poland
[35]Horia Hulubei National Institute of Physics and Nuclear Engineering, Bucharest-Magurele, Romania
[36]Petersburg Nuclear Physics Institute NRC Kurchatov Institute (PNPI NRC KI), Gatchina, Russia
[37]Institute of Theoretical and Experimental Physics NRC Kurchatov Institute (ITEP NRC KI), Moscow, Russia, Moscow, Russia
[38]Institute of Nuclear Physics, Moscow State University (SINP MSU), Moscow, Russia
[39]Institute for Nuclear Research of the Russian Academy of Sciences (INR RAS), Moscow, Russia
[40]Yandex School of Data Analysis, Moscow, Russia
[41]Budker Institute of Nuclear Physics (SB RAS), Novosibirsk, Russia
[42]Institute for High Energy Physics NRC Kurchatov Institute (IHEP NRC KI), Protvino, Russia, Protvino, Russia
[43]ICCUB, Universitat de Barcelona, Barcelona, Spain
[44]Instituto Galego de Física de Altas Enerxías (IGFAE), Universidade de Santiago de Compostela, Santiago de Compostela, Spain
[45]European Organization for Nuclear Research (CERN), Geneva, Switzerland
[46]Institute of Physics, Ecole Polytechnique Fédérale de Lausanne (EPFL), Lausanne, Switzerland
[47]Physik-Institut, Universität Zürich, Zürich, Switzerland
[48]NSC Kharkiv Institute of Physics and Technology (NSC KIPT), Kharkiv, Ukraine
[49]Institute for Nuclear Research of the National Academy of Sciences (KINR), Kyiv, Ukraine
[50]University of Birmingham, Birmingham, United Kingdom
[51]H.H. Wills Physics Laboratory, University of Bristol, Bristol, United Kingdom
[52]Cavendish Laboratory, University of Cambridge, Cambridge, United Kingdom
[53]Department of Physics, University of Warwick, Coventry, United Kingdom
[54]STFC Rutherford Appleton Laboratory, Didcot, United Kingdom
[55]School of Physics and Astronomy, University of Edinburgh, Edinburgh, United Kingdom
[56]School of Physics and Astronomy, University of Glasgow, Glasgow, United Kingdom
[57]Oliver Lodge Laboratory, University of Liverpool, Liverpool, United Kingdom
[58]Imperial College London, London, United Kingdom
[59]Department of Physics and Astronomy, University of Manchester, Manchester, United Kingdom
[60]Department of Physics, University of Oxford, Oxford, United Kingdom
[61]Massachusetts Institute of Technology, Cambridge, Massachusetts, USA
[62]University of Cincinnati, Cincinnati, Ohio, USA
[63]University of Maryland, College Park, Maryland, USA
[64]Los Alamos National Laboratory (LANL), Los Alamos, New Mexico, USA
[65]Syracuse University, Syracuse, New York, USA
[66]Laboratory of Mathematical and Subatomic Physics, Constantine, Algeria
[associated with Universidade Federal do Rio de Janeiro (UFRJ), Rio de Janeiro, Brazil]
[67]Pontifícia Universidade Católica do Rio de Janeiro (PUC-Rio), Rio de Janeiro, Brazil
[associated with Universidade Federal do Rio de Janeiro (UFRJ), Rio de Janeiro, Brazil]
[68]South China Normal University, Guangzhou, China
(associated with Center for High Energy Physics, Tsinghua University, Beijing, China)
[69]School of Physics and Technology, Wuhan University, Wuhan, China
(associated with Center for High Energy Physics, Tsinghua University, Beijing, China)
[70]Departamento de Fisica, Universidad Nacional de Colombia, Bogota, Colombia
(associated with LPNHE, Sorbonne Université, Paris Diderot Sorbonne Paris Cité, CNRS/IN2P3, Paris, France)
[71]Institut für Physik, Universität Rostock, Rostock, Germany
(associated with Physikalisches Institut, Ruprecht-Karls-Universität Heidelberg, Heidelberg, Germany)
[72]Van Swinderen Institute, University of Groningen, Groningen, Netherlands
(associated with Nikhef National Institute for Subatomic Physics, Amsterdam, Netherlands)

[73]National Research Centre Kurchatov Institute, Moscow, Russia
[associated with Institute of Theoretical and Experimental Physics NRC Kurchatov Institute (ITEP NRC KI), Moscow, Russia, Moscow, Russia]
[74]National University of Science and Technology "MISIS", Moscow, Russia
[associated with Institute of Theoretical and Experimental Physics NRC Kurchatov Institute (ITEP NRC KI), Moscow, Russia, Moscow, Russia]
[75]National Research University Higher School of Economics, Moscow, Russia
(associated with Yandex School of Data Analysis, Moscow, Russia)
[76]National Research Tomsk Polytechnic University, Tomsk, Russia
[associated with Institute of Theoretical and Experimental Physics NRC Kurchatov Institute (ITEP NRC KI), Moscow, Russia, Moscow, Russia]
[77]Instituto de Fisica Corpuscular, Centro Mixto Universidad de Valencia—CSIC, Valencia, Spain
(associated with ICCUB, Universitat de Barcelona, Barcelona, Spain)
[78]University of Michigan, Ann Arbor, Michigan, USA
(associated with Syracuse University, Syracuse, New York, USA)

[a]Deceased.
[b]Also at Laboratoire Leprince-Ringuet, Palaiseau, France.
[c]Also at Università di Genova, Genova, Italy.
[d]Also at Università di Bologna, Bologna, Italy.
[e]Also at Università di Modena e Reggio Emilia, Modena, Italy.
[f]Also at Novosibirsk State University, Novosibirsk, Russia.
[g]Also at Università di Ferrara, Ferrara, Italy.
[h]Also at Università di Milano Bicocca, Milano, Italy.
[i]Also at LIFAELS, La Salle, Universitat Ramon Llull, Barcelona, Spain.
[j]Also at Università di Pisa, Pisa, Italy.
[k]Also at Università di Bari, Bari, Italy.
[l]Also at INFN Sezione di Trieste, Trieste, Italy.
[m]Also at Università degli Studi di Milano, Milano, Italy.
[n]Also at Universidade Federal do Triângulo Mineiro (UFTM), Uberaba-MG, Brazil.
[o]Also at AGH—University of Science and Technology, Faculty of Computer Science, Electronics and Telecommunications, Kraków, Poland.
[p]Also at Lanzhou University, Lanzhou, China.
[q]Also at Università di Padova, Padova, Italy.
[r]Also at Università di Cagliari, Cagliari, Italy.
[s]Also at MSU—Iligan Institute of Technology (MSU-IIT), Iligan, Philippines.
[t]Also at Scuola Normale Superiore, Pisa, Italy.
[u]Also at Hanoi University of Science, Hanoi, Vietnam.
[v]Also at P.N. Lebedev Physical Institute, Russian Academy of Science (LPI RAS), Moscow, Russia.
[w]Also at Università di Roma Tor Vergata, Roma, Italy.
[x]Also at Università di Roma La Sapienza, Roma, Italy.
[y]Also at Università della Basilicata, Potenza, Italy.
[z]Also at Università di Urbino, Urbino, Italy.
[aa]Also at Physics and Micro Electronic College, Hunan University, Changsha City, China.
[bb]Also at School of Physics and Information Technology, Shaanxi Normal University (SNNU), Xi'an, China.